31st Annual International Conference of the IEEE EMBS
Minneapolis, Minnesota, USA, September 2-6, 2009

Efficacy of Noncontact Mapping in Detecting Epicardial Activation

Elnaz Shokrollahi [1,2], Sridhar Krishnan [1], Stéphane Massé [2], Karthikyan Umapathy[1,2], Luc Soucie [3], Talha A. Farid [2] and Kumaraswamy Nanthakumar[2]
Ryerson University[1], Toronto General Hospital[2], Toronto, St. Jude Medical[3], Missisauga, Canada

Abstract— **The aim of this study is to determine if some of the characteristics of reconstructed unipolar electrograms from the noncontact mapping system can be used to detect epicardial electrical activation in a canine heart. This would help the electrophysiologist know where exactly the origin or the critical point in tissue is located. Following this, arrhythmia can be successfully treated by ablating that part of the tissue of heart. Virtual electrograms were recorded while pacing the right ventricle of an open-chest dog at multiple endocardial and epicardial sites using the commercially available noncontact mapping system (EnSite 3000). The endocardial and epicardial paced virtual electrograms from the juxtaposing sites allow for analyzing systematically the differences in their morphologies. Maximal dV/dt, area under the depolarization curve and latency extracted from unipolar electrograms demonstrated significant difference between epicardial and endocardial pacing sites with a p-value of less than 0.01 in all three cases. The above features were fed to a linear discriminant analysis based classifier and high classification accuracy was achieved. In conclusion, reliable criteria can be proposed to allow for discrimination of an endocardial versus epicardial origin of electrical activation.**

Index Terms— **Noncontact mapping, Electrograms, Ventricular arrhythmia, Detection**

[1]

I. INTRODUCTION

In order to localize arrhythmias, conventional contact catheter mapping records the endocardial electrograms sequentially from a small, localized area of endocardium surface. As a consequence this technique is time consuming as endocardial electrograms are recorded sequentially, making mapping of complex cardiac arrhythmias difficult. Recently, a non-contact mapping system (EnSite, Endocardial Solutions, St. Paul, MN, USA) has been introduced and allowed improved mapping with the help in localizing the site of origin of sustained ventricular tachycardias. This will facilitate the surgical treatment of these arrhythmias [1], [2], [3], [4]. Understanding the complex ventricular arrhythmias result in more effective targeting of radio-frequency (RF) energy applications in patients with ventricular tachycardias [5], [6], [7], [8]. In this investigation, we show that the characteristics of the unipolar virtual electrograms recorded with EnSite system may help discern the epicardial origin of electrical activation. The performances of different signal features in discriminating endocardial/epicardial origins of electrical activation were assessed by comparing the area under the receiver operating characteristic (ROC) curves. The classification accuracy was estimated using the leave-one-out method [9]. The paper is organized into following sections. Section II covers the methodology, Section III presents results; Discussion and conclusion are provided in Section IV.

II. METHODS

A. Model Preparation

The dog was anaesthetized with sodium pentobarbital (30 mg/kg IV) and maintained with 1-2% isoflurane. The protocol was approved by the Animal Care Committee of St Michael's Hospital, Toronto (ON, Canada). The investigation conforms to the Guide for the Care and Use of Laboratory Animals, US National Institutes of Health (NIH Publication No. 85-23, revised 1996). Buprenorphine 0.3 mg IV was administered before starting any procedure. ECG leads I, II, and aVF and aortic blood pressure were monitored continuously using a VR12 physiological signal recorder (Electronics for Medicine, Pleasantville, NY, USA).

B. Noncontact Mapping

The technique of non-contact mapping has been described previously [10], [11]. Briefly; the system, EnSite 3000 (St. Jude Medical, St. Paul, MN, USA), consists of a catheter (9-French) with a multi-electrode array (MEA) surrounding a 7.5-ml balloon mounted at the distal end. The 9-French 64-electrode balloon catheter was passed over a guide wire into right ventricle (RV). Activation clotting time was maintained over 250 seconds with the use of Heparin. By moving the ablation catheter around endocardium, multiple spatial points were identified. An incorporated locator system was used in conjunction with fluoroscopy to position the conventional electrode catheter. A three-dimensional (3-D) RV geometry was generated by interpolation between the mapped sites and defining boundaries. By determining the catheter position from fluoroscopy and electrogram recordings anatomic structures were labeled on the 3-D geometry. The system calculates real-time endocardial potentials at more than 3000 virtual sites by using inverse solution mathematics. Simultaneous virtual unipolar electrograms were mathematically reconstructed and displayed on the anatomic model, producing isopotential or isochronal color maps. It is possible, at any given interval of the cycle, to display the virtual

[1]This document is submitted on April 23, 2009. E. Shokrollahi, S. Krishnan and K. Umapathy are with Ryerson University, Toronto, CA M5B 2K3. phone: +1647-822-6163; email: eshokrol@ee.ryerson.ca.
K. Nanthakumar, S. Massé,T. Farid, University Health Network, Toronto CA, Phone:1416-340-4442; email: kumar.nanthakumar@uhn.on.ca
L. Soucie, St. Jude Medical, Missisauga, CA, Phone: 613-298-6255; email: Lsoucie@sjm.com

unipolar endocardial electrograms from a chosen site of the endocardial surface [12].

A rectangular unipolar stimulus using basic drive cycle lengths of 350ms, 400ms, and 600ms cycle length was used to pace the heart. First, the pacing catheter was placed in different positions in the endocardium. The pacing amplitude was 0.5mV to 0.9V for different sites. The value was varied until the stimulus captured the ventricular conduction. The position of the pacing catheter was marked on the RV geometry. During the pacing, the noncontact array catheter records the endocardial electrograms for one minute. Fig. 1 shows an example of the endocardially paced electrogram. Following pacing several positions all around the RV, the pacing catheter was removed from the chamber and moved to the epicardium. For this iteration the pacing catheter was positioned on epicardial sites corresponding transmurally to the locations used on the endocardium. Fig. 1 also shows an example of epicardially paced electrogram superimposed on the endocardially paced electrogram. In order to capture the ventricular conduction and record it using the EnSite Array^{TM} catheter, the amplitude of pacing was a bit higher than the endocardial pacing sites. The recording for each site was again 1 minute. The data set therefore consisted of two sets of virtual electrograms: one set was obtained during endocardially pacing recorded with MEA. The second data set was obtained during epicardially paced and also recorded with MEA. The detected electrograms by the MEA were amplified and digitally transferred to a computer workstation. Fig. 2 shows the exact sites where the pacing took place.

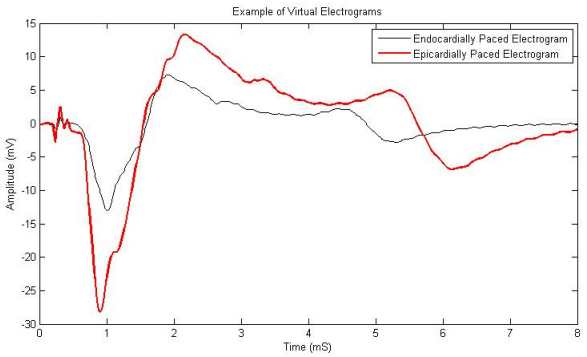

Fig. 1. Example of Electrogram paced Epicardially in solid thicker line and paced Endocardially in solid narrow line.

C. Signal Preprocessing

20 to 30 virtual electrogram recorded with both endocardial and epicardial pacing were selected for analysis and each data set was 4 seconds long. Since the pacing amplitude is different for endocardial and epicardial stimulus, therefore to make the chosen features independent from varying pacing electrograms each sample of the signal was divided by the square root of the energy of the signal. Energy of the signal was calculated for each $V(t)$ electrogram with the following equation.

$$E = \sum_{t=0}^{t=4} |V(t)|^2 \tag{1}$$

The virtual electrograms for each of the endocardially paced and epicardially paced signals were overlaid. In order to isolate the individual heart beat, signals recorded had to be segmented first. This segmentation was achieved manually (with approximately 780 samples in each segment) in such way that, each segment had only one cycle of the virtual electrogram. Moreover, in order to measure and detect the parameters used in this study (explained in Part D) the component between the pacing artifact and the depolarization part of virtual electrogram had to be segmented. This was done by having an imaginary line in mind (as base line) to separate the depolarization part from the rest of the signal. The high pass-filter was set at 8 Hz; all other filters were not changed (low-pass filter at IC 150 Hz, AutoFocus off, Spatial Filter off).

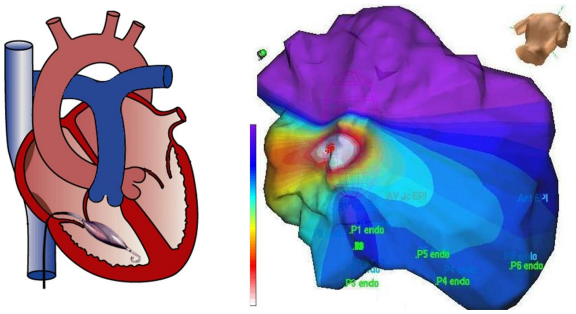

Fig. 2. Figure on Left is the position of the EnSite Array in the RV; Figure on Right: Illustration of the geometry and positions of the paced areas. This is color-coded isopotential map which shows the range of voltages across the RV at a given time; this is created by moving the ablation catheter around the RV geometry. At a nominal setting the purple represents *+5mV* (resting potential) and white represents *-5mV* (depolarization). The world-view reference is a user-selected torso which shows the exact position of the MEA in the chamber. The six paced points are demonstrated in green.

D. Analysis of Virtual Unipolar Electrograms

Because one of the pacing points had really different electrogram characteristic, we manually took it out of our data-set. After manual deletion of artifacts and electrograms with significantly different morphologies the following measurements were obtained for each $V(t)$ electrogram:

1) Peak Negative Voltage (PNV) in (mV): The lowest negative point on a wave. The peak negative voltage indicates the maximum negative voltage of the wave.

2) Maximal negative dV/dt (mV/ms): Greatest amplitude difference in voltage

$$dV/dt = \frac{V(t+h) - V(t)}{h} \tag{2}$$

where value of *h* close to zero will give a good approximation to the slope of the tangent line.

3) Area under the curve (AUC) from baseline crossing of

unipolar electrogram to maximal negative voltage,

$$AUC = 2 * \sum_{t=0}^{PNV} V(t) \tag{3}$$

4) Presence of an initial R-wave versus initial *QS* pattern: R-wave is the initial upward deflection of the *QRS complex*, following the Q-wave in the normal ECG and representing early depolarization of the ventricles. Clinicians mostly think of an acceptable R-wave to be ($\geq$ 5mV) [13].
5) Duration: Electrogram duration assessed from baseline crossing of the unipolar electrogram to PNV (ms).
6) Presence of low-amplitude depolarization preceding the spike of electrical activation of the local myocardium. When the mapping electrode is not in contact with the myocardium (noncontact mapping case) if the electrogram is a far-field signal generated by tissue some distance from the recording electrode, then the initial negative slope of the recording is typically slow. This is known in literature as "Blue Ghost" [14].
Fig. 3 shows an example of how the above features were calculated.

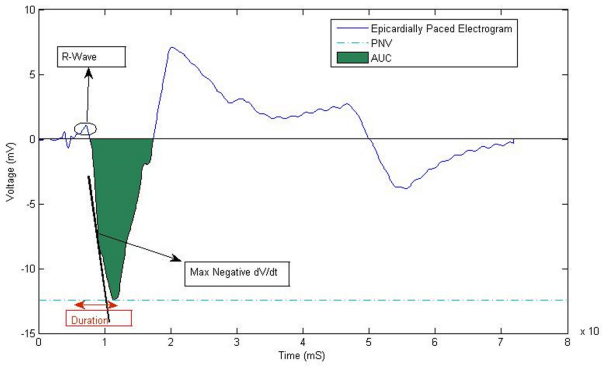

Fig. 3. Unipolar virtual electrogram paced epicardially. Features described in the text are shown on this electrogram.

E. ROC Analysis

Perhaps the simplest measure of diagnostic decision quality in the medical world is the fraction of cases for which the classification is correct; this is called "accuracy". To evaluate the performance of the signal features, receiver operating characteristic (ROC) curves were used. This will help to compare the discrimination of electrical activity of endocardial versus epicardial [15]. ROC curve is defined as a plot of test *sensitivity (SE)* as the y-coordinate versus its *1-specificity (SP)* or false positive rate as the x-coordinate. It is an effective method of evaluating the quality or performance of diagnostic tests. In this study, true positive (TP) is when the signal is correctly classified, i.e. epicardially paced electrogram classified as extra-stimulus signal. If the signal is classified as endocardially paced, it is false negative (FN). If the signal is endocardially paced and it is classified as an endocardial electrogram, it is true negative (TN), and false positive (FP) is defined similarly.

$$SE = \frac{TP}{TP + FN}, SP = \frac{TN}{FP + TN} \tag{4}$$

Given a classifier and a set of instances (the test set), a two-by-two confusion matrix can be constructed representing the dispositions of the set of instances.
The total area under the ROC curve is a measure of the performance of the diagnostic test since it reflects the test performance at all possible cut-off levels. The larger the area, the better the performance. The area under the ROC curves and their standard errors were derived by using SPSS (Statistical Package for the Social Sciences, Version 16.0.1, Chicago, IL, USA). [16].

F. Classification

The classification accuracy was estimated using the leave-one-out method. In leave-one-out method, one sample is excluded from the data-set and the classifier is trained with the remaining samples. Then the excluded signal is used as the test data and the classification accuracy is determined. This is repeated for all samples of the data-set. Since each signal is excluded from the training set in turn, the independence between the test and the training sets are maintained.

G. t−Test

The t−Test was used to compare the average of the amplitude values of the two signals. The result is presented in Table 1. If the noncontact mapping system revealed significant differences between the characteristics of endocardial or epicardial origin of activation, in Table 1 it is indicated as $p < 0.05$ or $p < 0.01$, otherwise non significant (NS).

III. RESULTS

Analyzing the PNV and duration of the virtual electrograms recorded with the MEA exhibit small differences between the endocardially and epicardially paced signals (t-test = NS). The Occurrence of R-wave and initial low amplitude depolarization in most of the epicardially stimulated electrograms were the good features for distinguishing the electrical activation ($P < 0.01$). The latency between the onset of the unipolar electrograms and pacing artifact differed significantly with the longer latency for the electrograms reconstructed during epicardial stimulus ($P < 0.01$). Area under the curve for the depolarization portion of the unipolar electrograms of the epicardially paced signals was wider than the endocardially paced. The parameters analyzed above are summarized in Table I. Data are given as mean $\pm$ SD.
ROC curves were used to compare the potentially reliable criteria. Each of the variables had an area under the ROC curves significantly above 0.5 indicating that all were good tests of distinction of activation.
Table II below summarize the classification for the best discriminator found: Latency.

TABLE I

ELECTROCARDIOGRAPHIC PARAMETERS ANALYZED

Case	Endocardial	Epicardial	t−Test
Latency	14.5±5.3*ms*	18.2±7.8 *ms*	$p < 0.01$
Duration	18.8±6.2 *ms*	22.2± 5.3 *ms*	NS
PNV	-2±1 *mV*	-3±5.3 *mV*	NS
Low Amp. Depo.	0 %	60%	$p < 0.05$
Max Neg. dV/dt	1.6±0.2 *mV/ms*	2.27±0.4 *mV/ms*	$p < 0.05$
AUC	881±36	1090±50.5	$p < 0.05$
R-Wave	0%	80%	$p < 0.01$

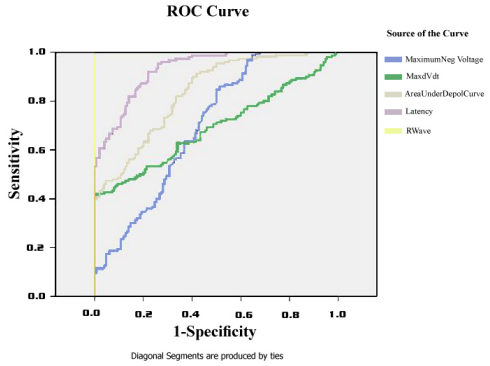

Fig. 4. ROC curve results. The area under the ROC curve for R-wave was 1, latency was 0.932, area under the depolarization curve was 0.833, maximum negative voltage was 0.698 and maximum dV/dt was 0.692.

IV. DISCUSSIONS AND CONCLUSIONS

Findings of this experiment may be discussed if these results obtained in the present study are still valid during the reentrant and focal arrhythmias and also if the experimental study can correspond well with clinical findings. Further studies would help to determine if differing characteristics is applicable to human ventricular tachycardia.

We have presented the electrographic parameters to analyze the difference between the endocardially paced and epicardially paced electrograms in this preliminary study. The morphologies of the unipolar electrograms generated by the noncontact mapping system allowed the discrimination of endocardial versus epicardial origin of activation. R-wave appeared to be the best discriminant feature between endocardially and epicardially paced electrograms. From statistical results, it might be possible to identify possible parameters to be used to discriminate between epicardial and endocardial activation. We also believe the possibility that the combinations of these criteria might improve the perception over any single criterion.This may allow detection of tachycardia that originates epicardially. It should be kept in mind that intracavitary maps deserve further studies, especially their performance should be evaluated in animal preparations of sustained ventricular tachycardias, as a preliminary step toward clinical trials

V. ACKNOWLEDGMENTS

The authors would like to acknowledge the early contribution of Andrew Ramadeen, Dr. Xudong Hu and Dr. Paul Dorian from St. Michael's Hospital in Toronto, Canada; and would like to thank Mr. Paymon Eskandanian.

Method	Groups	Endocardial	Epicardial	Total
Cross-validated	Endocardial	131	19	150
	Epicardial	35	115	150
%	Endocardial	**87.3**	12.7	100
	Epicardial	23.3	**76.7**	100

TABLE II

CROSS-VALIDATED: LINEAR DISCRIMINANT ANALYSIS WITH LEAVE-ONE-OUT METHOD, % - PERCENTAGE OF CLASSIFICATION.

REFERENCES

[1] C. Gornick, S. Adler, B. Pederson, J. Hauck, J. Budd, and J. Schweitzer, "Validation of a new noncontact catheter system for electroanatomic mapping of left ventricular endocardium," *Circulation*, vol. 99, no. 6, pp. 829–835, 1999.

[2] A. Kadish, J. Hauck, B. Pederson, G. Beatty, and C. Gornick, "Mapping of atrial activation with a noncontact, multielectrode catheter in dogs," *Circulation*, vol. 99, no. 14, pp. 1906–1913, 1999.

[3] N. Peters, W. Jackman, R. Schilling, G. Beatty, and D. Davies, "Human left ventricular endocardial activation mapping using a novel noncontact catheter," *Circulation*, vol. 95, no. 6, pp. 1658–1660, 1997.

[4] L. Gepstein, G. Hayam, and S. Ben-Haim, "A novel method for nonfluoroscopic catheter-based electroanatomical mapping of the heart In vitro and in vivo accuracy results," *Circulation*, vol. 95, no. 6, pp. 1611–1622, 1997.

[5] T. Betts, P. Roberts, S. Aelen, and J. Morgan, "Radiofrequency ablation of idiopathic left ventricular tachycardia at the site of earliest activation as determined by noncontact mapping," *Journal of Cardiovascular Electrophysiology*, vol. 11, no. 10, pp. 1094–1101, 2000.

[6] T. Paul, A. Blaufox, and J. Saul, "Non-contact mapping and ablation of tachycardia originating in the right ventricular outflow tract," *Cardiology in the Young*, vol. 12, no. 03, pp. 294–297, 2006.

[7] P. Dorostkar, J. Cheng, and M. Scheinman, "Electroanatomical mapping and ablation of the substrate supporting intraatrial reentrant tachycardia after palliation for complex congenital heart disease," *Pacing and Clinical Electrophysiology*, vol. 21, no. 9, pp. 1810–1819, 1998.

[8] F. P. Stevenson WG, Delacretaz E, "Identification and ablation of macro reentrant ventricular tachycardia with the CARTO electroanatomical mapping system," *Pacing and Clinical Electrophysiology*, vol. 21, pp. 1445–1456, 1998.

[9] K. Umapathy, S. Krishnan, and S. Jimaa, "Multigroup classification of audio signals using time-frequency parameters," *IEEE Transactions on Multimedia*, vol. 7, no. 2, pp. 308–315, 2005.

[10] Z. Jiangang and C. Kejiang, "Endocardial mapping and ablation of tachycardia guided by noncontact balloon catheter mapping system," *Chinese medical journal*, vol. 115, no. 6, pp. 909–913, 2002.

[11] C. Gornick, S. Adler, B. Pederson, J. Hauck, J. Budd, and J. Schweitzer, "Validation of a new noncontact catheter system for electroanatomic mapping of left ventricular endocardium," *Circulation*, vol. 99, no. 6, pp. 829–835, 1999.

[12] P. Della Bella, A. Pappalardo, S. Riva, C. Tondo, G. Fassini, and N. Trevisi, "Non-contact mapping to guide catheter ablation of untolerated ventricular tachycardia," *European heart journal*, vol. 23, no. 9, pp. 742–752, 2002.

[13] M. Kroll, T. Kriebel, B. Windhagen-Mahnert, B. Franzbach, C. Jux, M. Zutz, J. Tebbenjohanns, and T. Paul, "Differentiation by Electrogram Characteristics Using the Noncontact Mapping System," *Pacing and Clinical Electrophysiology*, vol. 26, no. 10, pp. 1970–1978, 2003.

[14] W. Whitwam, S. Rule, and S. Narayan, "Noncontact mapping of small pulmonary artery potentials preceding ectopy from the right ventricular outflow tract," *Heart Rhythm*, vol. 4, no. 7, pp. 959–963, 2007.

[15] C. Metz, "Basic principles of ROC analysis." vol. 8, no. 4, p. 283, 1978.

[16] S. Inc., "SPSS advanced statistics user's guide," 1990.